European Journal of Nuclear Medicine and Molecular Imaging (2019) 46:467–477
https://doi.org/10.1007/s00259-018-4210-1

ORIGINAL ARTICLE

Prognostic impact of combining whole-body PET/CT and brain PET/MR in patients with lung adenocarcinoma and brain metastases

Kung-Chu Ho[1] · Cheng-Hong Toh[2] · Shih-Hong Li[3] · Chien-Ying Liu[3] · Cheng-Ta Yang[3] · Yu-Jen Lu[4] · Tzu-Pei Su[1] · Chih-Wei Wang[5] · Tzu-Chen Yen[6,7]

Received: 11 September 2018 / Accepted: 2 November 2018 / Published online: 10 November 2018

Abstract

Purpose The role of brain FDG-PET in patients with lung cancer and brain metastases remains unclear. Here, we sought to determine the prognostic significance of whole-body PET/CT plus brain PET/MR in predicting the time to neurological progression (nTTP) and overall survival (OS) in this patient group.

Methods Of 802 patients with non-small cell lung cancer who underwent primary staging by a single-day protocol of whole-body PET/CT plus brain PET/MR, 72 cases with adenocarcinoma and brain metastases were enrolled for a prognostic analysis of OS. On the basis of the available follow-up brain status, only 52 patients were eligible for prognostic analysis of nTTP. Metastatic brain tumors were identified on post-contrast MR imaging, and the tumor-to-brain ratio (TBR) was measured on PET images.

Results Multivariate analysis revealed that FDG-PET findings and eligibility for initial treatment with targeted therapy were significant independent predictors of nTTP and OS. A new index, termed the molecular imaging prognostic (MIP) score, was proposed to define three disease classes. MIP scores were significant predictors of both nTTP and OS ($P < 0.001$). Pre-existing prognostic indices such as Lung-molGPA scores were significant predictors of OS but did not predict nTTP.

Conclusions When staging is performed with whole-body PET/CT plus brain PET/MR, our new prognostic index may be helpful to stratify the outcomes of patients with lung adenocarcinoma and brain metastases. The superior prognostic power of this index for nTTP might be used to select appropriate patients for intracranial control and thereby achieve better quality of life.

Keywords Lung adenocarcinoma · Brain metastasis · PET/CT · PET/MR

✉ Tzu-Chen Yen
yentc1110@gmail.com

[1] Department of Nuclear Medicine, Chang Gung Memorial Hospital and Chang Gung University, Keelung, Taiwan

[2] Department of Medical Imaging and Intervention, Chang Gung Memorial Hospital and Chang Gung University, Taoyuan, Taiwan

[3] Department of Thoracic Medicine, Chang Gung Memorial Hospital and Chang Gung University, Taoyuan, Taiwan

[4] Department of Neurosurgery, Chang Gung Memorial Hospital and Chang Gung University, Taoyuan, Taiwan

[5] Department of Anatomic Pathology, Chang Gung Memorial Hospital and Chang Gung University, Taoyuan, Taiwan

[6] Department of Nuclear Medicine and Center for Advanced Molecular Imaging and Translation, Chang Gung Memorial Hospital and Chang Gung University, 5 Fu-Shin Street, Kueishan, Taoyuan 333, Taiwan

[7] Department of Nuclear Medicine, Xiamen Chang Gung Hospital, Xiamen, Fujian, China

Introduction

The occurrence of brain metastases (BMs) is higher in lung malignancies compared with other solid neoplasms [1–3]. In a population-based study, the incidence of BM at initial presentation in non-small cell lung cancer (NSCLC) was higher than that observed in small cell lung cancer. Among NSCLCs, the highest incidence was noted in adenocarcinomas [2]. Approximately 36% of all lung cancer patients were found to develop BMs over the course of the disease [4]. Notably, the incidence of BMs in patients with non-metastatic NSCLC was 9% [5].

FDG-PET/CT imaging, which is commonly used to evaluate the extent of disease and to provide accurate staging of NSCLC, is recommended by National Comprehensive Cancer Network (NCCN) guidelines for stage I to stage IV disease [6]. Moreover, contrast-enhanced brain MRI should be performed to rule out the presence of metastases in NSCLC patients who are candidates for aggressive multimodal therapies.

Brain MRI is recommended for patients with stage II to IV disease and is optional for patients with stage IB [6]. An accurate identification of the number, location, and size of BMs on brain MRI images is paramount to allocate the interventions that would be more appropriate for the patients [7]. Intriguingly, contrast-enhanced MR has been consistently shown to be superior to both contrast-enhanced CT and non-enhanced MR [8].

Difficulties in promptly scheduling appointments for MRI examinations are not uncommon, and reducing barriers to a timely MR imaging schedule is a critical issue [9]. Several recent studies have shown a similar lung cancer staging ability for PET/CT and PET/MR imaging [10–13]. Thus, it is reasonable to use PET/MR for lung cancer staging as both body PET and brain MRI information can be obtained in a single examination. However, the much longer PET/MR examination time (i.e., 1–1.5 h) remains a major obstacle for its routine use in clinical practice [10, 11]. Moreover, post-contrast scans in whole-body PET/MR imaging are focused on the thorax (without dedicated protocols for the brain within the limited scanning time) [11, 13]. To obtain high-quality brain MRI data with standard PET staging, we developed a staging protocol for patients with NSCLC that combines the use of whole-body FDG-PET/CT and brain PET/MR. Because in our hospital the PET/MR and PET/CT scanners are located in the same department, the scanning schedule of the two modalities could be arranged on the same day.

Although the average survival for patients with BM is typically less than 6 months, certain cases can experience a longer survival [14]. In addition, an early aggressive treatment—comprehensively including surgery, radiotherapy, and targeted therapy—can improve the patient's functional status and prolong disease control as well as survival [15]. The Diagnosis-Specific Graded Prognostic Assessment (DS-GPA) is a prognostic index that uses patient age, Karnofsky Performance Status (KPS), presence of extracranial metastases, and number of BMs to define four disease classes [16]. The original DS-GPA was developed between 1985 and 2005 (i.e., before the era of targeted therapy) in patients with NSCLC and BM. To update this index by incorporating genetic and molecular data, a new index—termed the Lung-molGPA—has been developed between 2006 and 2014 [17]. The significant prognostic factors in the new index include the original four factors used in the DS-GPA index plus gene mutation status (EGFR- or ALK-positivity) in patients with adenocarcinoma.

Although the routine staging of brain status in patients with NSCLC is based on brain contrast-enhanced MRI [6], brain PET/CT shows more than 70% sensitivity for detecting BMs in lung cancer and a high specificity [18]. Patients with FDG-PET defined stage IV NSCLC and single-organ metastases (including BMs) have been shown to have a favorable prognosis [19]. Importantly, FDG uptake of the primary lung tumor is known to have prognostic value in NSCLC [20, 21]. However, there are no available data in the literature regarding the prognostic value of brain FDG-PET in lung cancer patients with BMs. Starting from these premises, we sought to clarify the prognostic role of brain FDG-PET in NSCLC patients with BM. Specifically, we designed this retrospective study to investigate the potential value of a single-day protocol of whole-body PET/CT plus brain PET/MR.

Materials and methods

Patients

Between December 2014 and June 2017, a total of 802 patients underwent primary staging for NSCLC with whole-body FDG-PET/CT plus brain PET/MRI at the Chang Gung Memorial Hospital. In this retrospective study, we enrolled patients with primary NSCLC and newly diagnosed BM. Patients with recurrent brain disease were not included. A total of 79 patients with available clinical follow-up data were analyzed. Because the number of cases of non-adenocarcinoma ($n = 7$) was less than 10% of the study cohort, only cases showing adenocarcinoma ($n = 72$) as the major histological type were included in further analyses to investigate the prognostic significance of PET. The flowchart of patient assessments in the study is illustrated in Fig. 1. This was a single-center study, and the Institutional Review Board of the Chang Gung Memorial Hospital approved the study protocol (IRB 201700703B0).

Whole-body FDG-PET/CT image acquisition

Patients were required to fast for at least 4 h before examination, and blood glucose levels were < 200 mg/dl in all participants. No intravenous contrast enhancement was used. Patients underwent an intravenous injection of 370–555 MBq ^{18}F-FDG (depending on body weight), and images were acquired 60 min after its administration. Whole-body PET emission scans were performed from the skull vertex to the mid-thigh, without position changes. FDG-PET/CT imaging was conducted on a Biograph mCT scanner (Siemens Medical Solutions, Malvern, PA, USA). Low-dose CT images were used for attenuation correction of the PET data. PET images were reconstructed using a CT-based attenuation correction with an ordered-subset expectation maximization (OSEM) iterative reconstruction algorithm (two iterations and 21 subsets). Our site receives a SNM Clinical Trials Network certificate upon validation of a scanner.

Brain PET/MR

Brain PET/MR examinations were performed on a Biograph mMR (Siemens Healthcare, Erlangen, Germany) unit with a

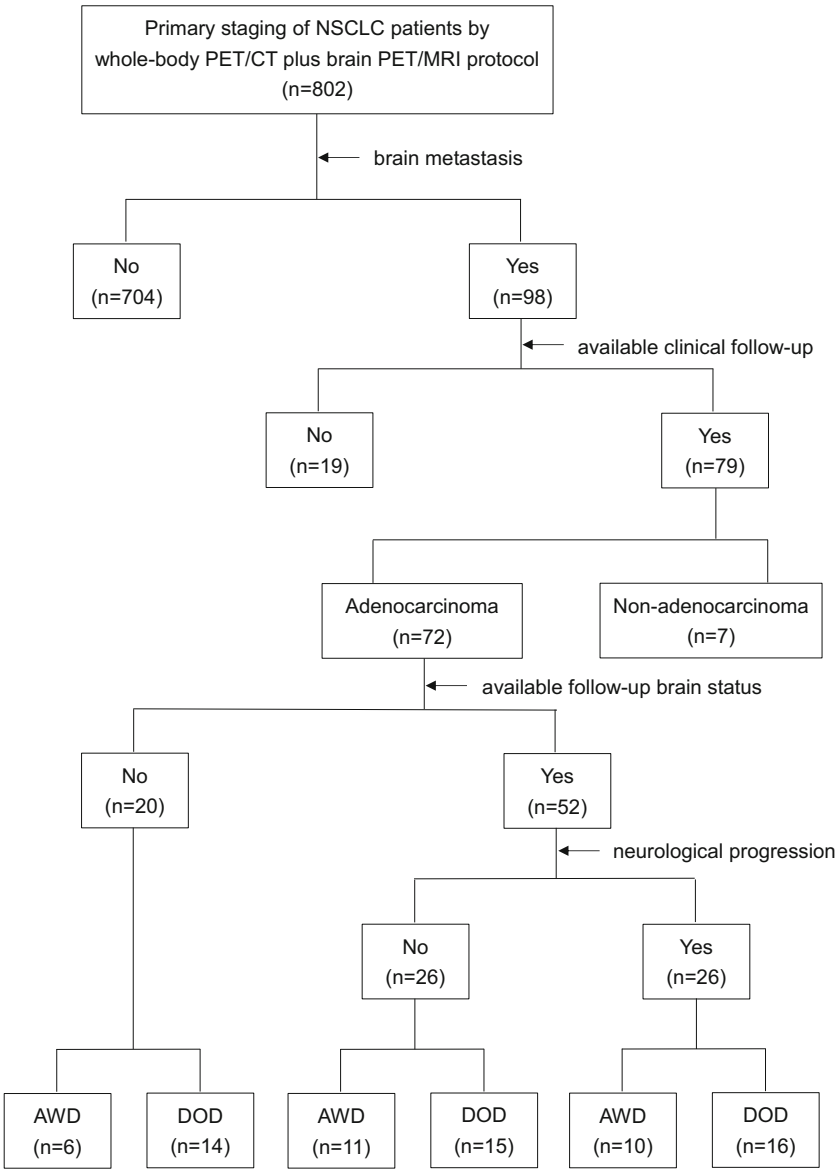

Fig. 1 Flowchart depicting the use of whole-body PET/CT plus brain PET/MR for staging patients with non-small cell lung cancer and brain metastases. *NSCLC* non-small cell lung cancer, *DOD* died of disease, *AWD* alive with disease

3-T magnetic field strength. In the MR imaging protocol for the 3-T scanner, the typical pulse sequences included transverse T1WI (TR/TE, 250/2.46 ms; section thickness, 4 mm; gap, 0 mm; matrix, 256 × 224; and FOV, 220 × 192.5 mm), transverse TSE T2WI (TR/TE, 4000/92 ms; section thickness, 4 mm; gap, 0; flip angle, 120°; turbo factor, 17; matrix, 512 × 314; and FOV, 220 × 192.5 mm), and transverse FLAIR (TR/TE/TI, 8200/87/2500 ms; section thickness, 4 mm; gap, 1 mm; matrix, 320 × 230; and FOV, 210 × 189 mm). After intravenous administration of the paramagnetic contrast agent, post-contrast MRI was conducted with transverse and coronal T1WI (TR/TE, 764/2.46 ms; section thickness, 4 mm; gap, 0 mm; matrix, 256 × 224; and FOV, 220 × 192.5 mm).

When ^{18}F-FDG was produced by the cyclotron and was available before the scheduled MRI scans, static FDG-PET data were acquired as the MRI acquisition started. Simultaneous FDG-PET/MR data acquisition started 30 min following the injection of FDG [22]. PET images were acquired in sinogram mode for 10 min, with a matrix size of 344 × 344, reconstruction with the OSEM algorithm (21 subsets, three iterations), and post-filtering with a full-width half-maximum Gaussian kernel of 2 mm. Attenuation correction was performed using MR-based attenuation maps derived from ultrashort echo-time (UTE) MR sequences (TR/TE1/TE2, 11.94/0.07/2.46 ms; section thickness, 1.56 mm; flip angle, 10°; and FOV, 300 × 300 mm) [23]. After brain PET/MR acquisition, the patients were transferred to the PET/CT scanner for the whole-body survey.

When ^{18}F-FDG produced by the cyclotron was not available before scheduled MRI scanning, only brain MR imaging was performed on the PET/MR scanner without acquiring brain PET data. The patients were then transferred to the

PET/CT room for FDG injections and whole-body scans on the same day.

Imaging analysis of brain metastases

Brain metastases were identified on post-contrast T1-weighted MR images by an experienced neuroradiologist. Both PET/CT and PET/MR images were analyzed on a dedicated workstation (syngo TrueD; Siemens Healthcare). Brain PET/MR fusion images were automatically coregistered with the simultaneously acquired PET and MRI data. When FDG was not injected before the MR scan, manual coregistration of MRI and brain images from the PET/CT data was performed by the syngo TrueD software on the workstation. The PET volume of interest (VOI) was determined on PET/MR fusion images by post-contrast MRI to identify tumor volume (Fig. 2).

The standardized uptake value (SUV) for each voxel on PET was calculated as follows: SUV = (measured activity concentration [Bq/ml])/(injected activity [Bq]/body weight [kg] × 1000). As far as the assessment of the maximal tumor-to-brain ratio (TBR) is concerned, the maximal SUV of the tumor VOI was divided by the mean background activity in the healthy contralateral hemisphere [24]. A threshold TBR ≥ 1.6 was used to define positive FDG-PET findings for brain metastases [24, 25].

Treatment and patient evaluation

The treatment planning was made by the lung cancer team after completion of all pretreatment evaluation including whole-body PET/CT and brain PET/MR in our hospital. Disease was staged according to seventh edition AJCC staging in this time period [26]. Patients with positive EGFR mutation status—i.e., carrying an L858R (exon 21) or del19 (exon 19) mutation—were treated with either first- or second-generation tyrosine kinase inhibitors (TKI) as first-line therapy. Patients harboring EGFR mutations with exon 20 insertion received standard chemotherapy instead of targeted therapy. Patients with ALK-rearranged tumors were treated using ALK inhibitors. Patients without gene mutations received standard chemotherapy with pemetrexed and cisplatin. Immunotherapy was performed if the tumor showed high levels of PDL-1 expression. Patients underwent whole-brain radiotherapy depending on the clinical situation, such as those showing neurological symptoms. Post-treatment disease status was assessed using CT and/or FDG-PET imaging. The time intervals between each follow-up visit were 3 months for the first 7 years and 6–12 months thereafter. Brain MRI or CT scans were also performed for follow-up evaluations of the central nervous system upon completion of whole-brain radiotherapy or in the presence of symptoms suggestive of BMs.

Statistical analysis

The following variables were retrieved from clinical records: age at diagnosis, sex, smoking history, Eastern Cooperative Oncology Group (ECOG) performance status, presence of extracranial metastases, number and size of BMs, gene mutation status, initial treatment modalities, and clinical outcomes. The time to neurological progression (nTTP) and overall survival (OS) served as the main outcome measures. We calculated nTTP from the initial date of local or systemic treatment

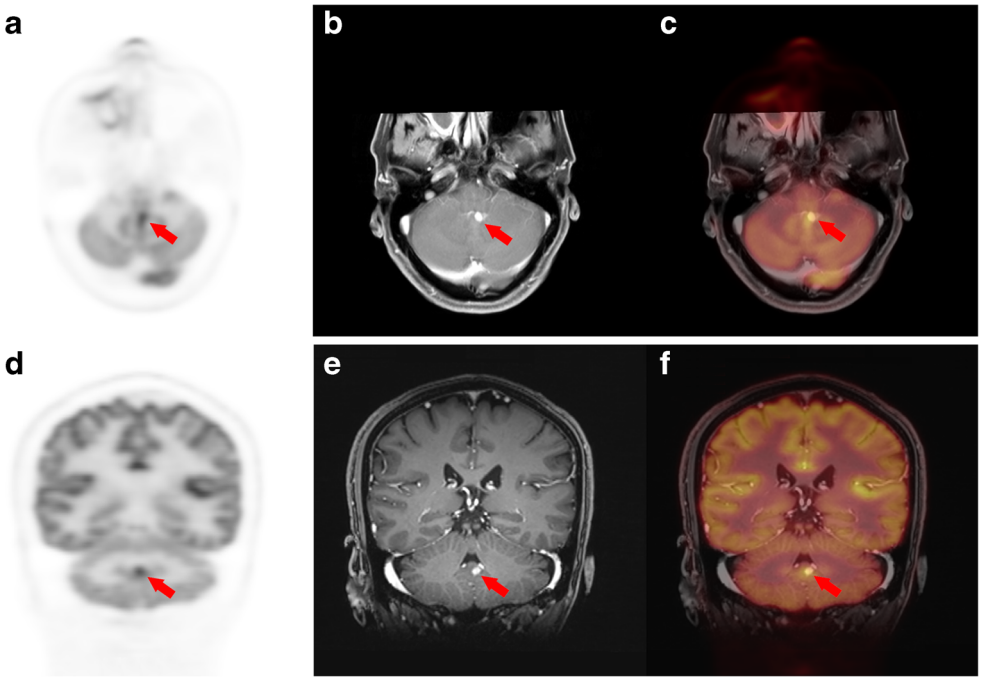

Fig. 2 Illustration showing brain tumors with the smallest size in the positive PET group (*red arrow*). The tumor size measured on post-contrast T1-weighted MR imaging was 0.6 cm. The tumor volume of interest (VOI) on PET (**a**) (**d**) was determined on PET/MR fusion images (**c**) (**f**) by post-contrast MRI identified tumor volume (**b**) (**e**). As far as the assessment of the maximal tumor-to-brain ratio (TBR) is concerned, the maximal SUV of the tumor VOI was divided by the mean background activity in the healthy contralateral hemisphere. The TBR in this case was 2.2; a TBR ≥ 1.6 was considered as positive

to the date of radiological progression of BMs. OS was defined as the time elapsed from the date of diagnosis to the date of death from any cause or censored on the date of the last follow-up. Survival curves were constructed with the Kaplan–Meier method and compared using the log-rank test. Univariate survival analyses were carried out using the Cox proportional hazards regression method. A multivariate regression model was constructed using the Cox proportional hazards regression method with a forward stepwise selection procedure. All variables included in univariate analysis were entered as potential covariates in the multivariate model. Data were analyzed using the SPSS 18.0 statistical package (SPSS Inc., Chicago, IL, USA). Two-tailed P values < 0.05 were considered statistically significant.

A new index termed the molecular imaging prognostic (MIP) score was proposed to define disease classes, using significantly independent predictors of nTTP and OS identified in the multivariate analysis. For comparisons with the pre-existing Lung-molGPA prognostic index for adenocarcinoma, five factors (patient age, performance status, presence of extracranial metastases, number of BMs, and gene mutation status) were used to define four disease classes [17]. ECOG values were transformed to KPS scores for determining the performance status.

Results

Incidence of BMs in NSCLC

Among 802 patients with NSCLC, 208 were stage I (26%), 62 were stage II (8%), 192 were stage III (24%), and 340 were stage IV (42%), including 79 BMs based on PET/CT and brain PET/MR results. Among 79 patients with BMs (72 adenocarcinoma, seven non-adenocarcinoma), 18 patients (16 adenocarcinoma, two squamous cell carcinoma) were upstaged from M0 to M1b in the presence of brain PET/MR. For overall stage excluding BM, two would be stage IB, two would be stage II, and 14 would be stage III. In the other 61 stage IV patients with BM, seven patients were upstaged from M1a to M1b by brain PET/MR. Based on assumed stage prior to brain PET/MR, BMs occurred in 1% (2/210) of stage I patients, 3% (2/64) of stage II patients, 7% (14/206) of stage III patients, and 19% (61/322) of stage IV patients.

Patients with lung adenocarcinoma and BMs

In this retrospective study of NSCLC cases, 91% (72/79) of BMs occurred in patients with adenocarcinomas. Seventy-two cases with adenocarcinomas and BMs were analyzed in relation to OS. Among these, only 52 patients had available follow-up brain images to define their neurological progression status (Table 1). There were no follow-up brain MRI or CT images available for the remaining 20 patients, including nine who died within 3 months after diagnosis. Table 2 depicts the general characteristics of the entire study cohort. There were 47 patients (65%) with gene mutations (EGFR- or ALK-positive status) and 43 patients (60%) who received initial treatment with targeted therapy (afatinib, 27; erlotinib, 12; gefitinib, two; crizotinib, one; and ceritinib, one). Patients carrying exon 20 inversion in the EGFR gene were not treated with TKI. Among the 29 patients who did not receive targeted therapy, 25 were treated with chemotherapy (either with or without brain radiotherapy), three with palliative brain radiotherapy only, and one with immunotherapy (pembrolizumab). A total of 31 patients underwent radiotherapy for BMs, including 13 who were treated with both radiotherapy and targeted therapy.

Brain FDG-PET imaging

Brain PET/MR fusion images were automatically coregistered with simultaneously acquired MRI and PET data started 30 min after injection in 43 patients. In another 29 cases, FDG was not injected before the MR scan, and coregistration of MRI acquired on PET/MR and brain images from PET/CT data acquired 60 min after injection was performed manually. By visual assessment on FDG-PET images, no metastatic brain tumor with TBR < 1.6 was identifiable.

Among the 21 patients showing positive PET findings for brain tumors, the mean TBR was 2.6 ± 0.8 (range, 1.6–4.1) and the mean size was 1.8 ± 1.2 cm (range, 0.6–5.5 cm). The smallest brain tumor showing positive PET findings was 0.6 cm in size (Fig. 2). The mean TBR were different between automatically coregistered images (2.8 ± 0.8, range, 1.6–4.1, $n = 15$) and manually coregistered images (2.0 ± 0.4, range, 1.6–2.6, $n = 6$) ($P = 0.035$). Among the 51 brain tumors showing negative PET findings, the mean TBR was 1.3 ± 0.2 (range, 0.9–1.57) and the mean size was 0.9 ± 0.7 cm (range, 0.2–4.5 cm). There was no significant difference of TBR between automatically coregistered images (1.3 ± 0.2, range, 0.9–1.57, $n = 28$) and manually coregistered images (1.3 ± 0.1, range, 1.0–1.54, $n = 23$).

Time to neurological progression and prognostic factors

Among the patients with follow-up data related to their brain status, 50% (26 of 52) showed progression of BMs. The results of univariate analysis identified the following significant prognostic factors for nTTP: gene mutation status, FDG-PET, and initial treatment with targeted therapy ($P < 0.05$; Table 1). Multivariate analysis revealed that FDG-PET and initial treatment with targeted therapy retained their independent

Table 1 General characteristics and analysis of the time to neurological progression in patients with available follow-up brain status data ($n = 52$)

Characteristic	n (%)	Univariate Cox regression analysis		Multivariate Cox regression analysis	
		Hazard ratio (95% CI)	P value	Hazard ratio (95% CI)	P value
Sex		1.41 (0.63–3.15)	0.399		
Female	26 (50)				
Male	26 (50)				
Age, years		1.14 (0.49–2.66)	0.766		
Range	38–92 (61)				
≥ 70 years	14 (27)				
Performance status		1.92 (0.64–5.77)	0.236		
ECOG 0–1 vs. ECOG 2–3	45 (87) / 7 (13)				
Extracranial metastases	37 (71)	1.21 (0.51–2.86)	0.661		
Gene mutations	35 (67)	0.41 (0.18–0.94)	0.030		
Brain metastases number		0.96 (0.71–1.30)	0.931		
1 vs. 2 vs. 3 vs. ≥ 4	18 (34) / 6 (12) / 6 (12) / 22 (42)				
Brain metastases size		1.28 (0.57–2.84)	0.547		
< 1 cm vs. ≥ 1 cm	29 (56) / 23 (44)				
Smoking	17 (32)	1.05 (0.70–1.60)	0.807		
FDG-PET		2.53 (1.06–6.04)	0.030	4.20 (1.63–10.85)	0.003
TBR < 1.6 vs. TBR ≥ 1.6	39 (75) / 13 (25)				
Initial treatment with targeted therapy	32 (62)	0.31 (0.14–0.69)	0.003	0.21 (0.08–0.51)	0.001
Initial treatment with radiotherapy	22 (42)	0.92 (0.41–2.04)	0.827		

ECOG Eastern Cooperative Oncology Group, *TBR* tumor-to-brain ratio, *CI* confidence interval

prognostic significance for nTTP ($P = 0.003$ and $P = 0.001$, respectively).

Overall survival and prognostic factors

In the entire study cohort ($n = 72$), 45 and 27 patients died of disease and were alive with disease, respectively. The results of univariate analysis identified the following significant prognostic factors for OS: performance status, gene mutation status, and initial treatment with targeted therapy ($P < 0.05$; Table 2). Multivariate analysis revealed that performance status, FDG-PET findings, and initial treatment with targeted therapy were independent predictors of OS ($P = 0.052$, $P = 0.035$, and $P < 0.001$, respectively).

Molecular imaging prognostic score versus the Lung-molGPA score

The two factors (FDG-PET and eligibility for initial treatment with targeted therapy), both of which were significantly independent predictors of both nTTP and OS, were combined to yield a new index termed MIP score and define three disease classes. Table 3 depicts the MIP scoring chart in patients with lung adenocarcinoma and BMs. The median nTTP and OS corresponding to MIP scores of 0, 1, and 2 were 9.1, 15.0, and 29.2 months and 4.5, 16.0, and 30.9 months, respectively. In comparison to a single factor, the median nTTP and OS corresponding to eligibility for initial treatment with targeted therapy (negative versus positive) were 9.9 versus 23.3 months and 10.5 versus 24.3 months, respectively.

An MIP score of 2 reflects the best prognosis, whereas a MIP score of 0 poses a higher risk - with hazard ratios of 21.46 (95% CI: 4.48–102.81) and 10.37 (95% CI: 3.54–30.34) for nTTP and OS, respectively (Table 4; Fig. 3). MIP scores were significant predictors of both nTTP and OS ($P < 0.001$; Fig. 4a and c). Lung-molGPA scores were found to predict OS ($P < 0.001$; Fig. 4d) but not nTTP (Fig. 4b).

Discussion

The prognostic impact of brain FDG-PET in patients with lung cancer and BMs has not been previously investigated. Intriguingly, current guidelines recommend PET/CT scanning from the skull base (i.e., saving the brain region) [6]. In this study, we reported for the first time the prognostic impact of brain FDG-PET using a single-day protocol combining whole-body PET/CT and brain PET/MR. A new prognostic index, termed MIP score, was proposed to predict OS and nTTP in patients with lung adenocarcinoma and BMs. The MIP score consisted of two factors, i.e., brain FDG-PET findings and eligibility for initial treatment with targeted therapy.

Table 2 Patient characteristics and analysis of overall survival in the entire study cohort ($n = 72$)

Characteristic	n (%)	Univariate Cox regression analysis		Multivariate Cox regression analysis	
		Hazard ratio (95% CI)	P value	Hazard ratio (95% CI)	P value
Sex		1.64 (0.90–3.00)	0.102		
Female	33 (46)				
Male	39 (54)				
Age, years		1.30 (0.67–2.53)	0.435		
Range (median)	38–92 (62)				
≥ 70 years	22 (31)				
Performance status		2.95 (1.47–5.93)	0.001	2.05 (1.00–4.21)	0.052
ECOG 0–1 vs. ECOG 2–3	59 (82) / 13 (18)				
Extra-cranial metastases	49 (68)	1.72 (0.85–3.48)	0.128		
Gene mutations	47 (65)	0.35 (0.19–0.63)	< 0.001		
Brain metastases number		1.16 (0.92–1.47)	0.349		
1 vs. 2 vs. 3 vs. ≥ 4	23 (32) / 10 (14) / 7 (10) / 32 (44)				
Brain metastases size		1.04 (0.57–1.87)	0.909		
<1 cm vs. ≥ 1 cm	41 (57) / 31 (43)				
Smoking	23 (32)	1.14 (0.82–1.58)	0.443		
FDG-PET		1.56 (0.83–2.91)	0.160	2.11 (1.05–4.21)	0.035
TBR < 1.6 vs. TBR ≥ 1.6	51 (71) / 21 (29)				
Initial treatment with targeted therapy	43 (60)	0.31 (0.17–0.57)	< 0.001	0.267 (0.14–0.52)	< 0.001
Initial treatment with radiotherapy	31 (43)	0.77 (0.42–1.40)	0.388		

ECOG Eastern Cooperative Oncology Group, *TBR* tumor-to-brain ratio, *CI* confidence interval

Because our hospital is equipped with both PET/CT and PET/MR scanners located in the same department, we were able to finalize the primary staging of NSCLC in a single day by combining whole-body PET/CT and brain PET/MR. This protocol offers several potential advantages, as follows: (1) the scanning time (12 min for PET/CT and 30 min for dedicated brain PET/MR) is comfortable and provides an efficient single-day clinical routine; (2) instead of the post-contrast scan focused on the thorax (required by whole-body PET/MR without dedicated brain MRI) [11, 13], we were able to obtain high-quality brain images during lung cancer staging; (3) PET/MR allows an accurate imaging analysis of metastatic brain tumors on PET; in addition, tumor VOI on PET can be easily identified on PET/MR fusion images using post-contrast MRI. We proposed a clinically efficient protocol for hospitals equipped with PET/CT and PET/MR scanners. However, our experience of manual coregistration of pure MRI acquired on PET/MR and brain images from PET/CT data suggested that it also works out in hospitals where these facilities are not in the same department.

Table 3 Scoring chart of the molecular imaging prognostic score in patients with lung adenocarcinoma and brain metastases

Prognostic factor	Score	
	0	1
FDG-PET TBR < 1.6	No	Yes
Eligibility for initial treatment with targeted therapy	No	Yes

TBR tumor-to-brain ratio

Although brain MRI is recommended in stage II–IV disease and optional in stage IB disease by NCCN guidelines [6], we included all patients with NSCLC to establish our local data of brain metastasis in lung cancer based on new modalities of both PET/CT and brain PET/MR. Recently, one report from an Australian group reported the results of brain metastasis screening in 718 patients with NSCLC staged using PET/CT and contrast-enhanced brain CT ($n = 703$) or MRI ($n = 15$). BMs were found in 0.5% (1/196) of stage I patients, 1% (1/104) of stage II patients, 1.6% (4/249) of stage III patients, and 7.3% (12/164) of stage IV patients [27]. In the present study of 802 patients with NSCLC, BMs occurred in 1% of stage I patients, 3% of stage II patients, 7% of stage III patients, and 19% of stage IV patients—based on assumed stage prior to brain PET/MR. Much higher BM incidence in our study cohort was most likely due to the use of brain MRI instead of CT for BM detection.

In this study, we were unable to perform simultaneous FDG-PET and MRI on PET/MR in all participants. Pure

Table 4 Cox proportional hazard analysis of molecular imaging prognostic score

Score	Time to neurological progression		Overall survival	
	Hazard ratio (95% CI)	*P* value	Hazard ratio (95% CI)	*P* value
0	21.46 (4.48–102.81)	< 0.001	10.37 (3.54–30.34)	< 0.001
1	4.30 (1.56–11.83)		2.93 (1.41–6.08)	
2	Reference category		Reference category	

CI confidence interval

MRI on PET/MR was scheduled to increase patient throughput. Brain PET/MR fusion images were automatically coregistered in 43 patients, whereas manual co-registration with dedicated software was performed in 29 cases. Imaging coregistration was so important that visual correlation might not be sufficient to identify small lesions or tumors with relatively lower TBR on brain FDG-PET. Despite a non-uniform protocol, our results suggest that manual coregistration of whole-body PET/CT and brain MRI is feasible when PET/MR is not available. Because there were no quantitative data

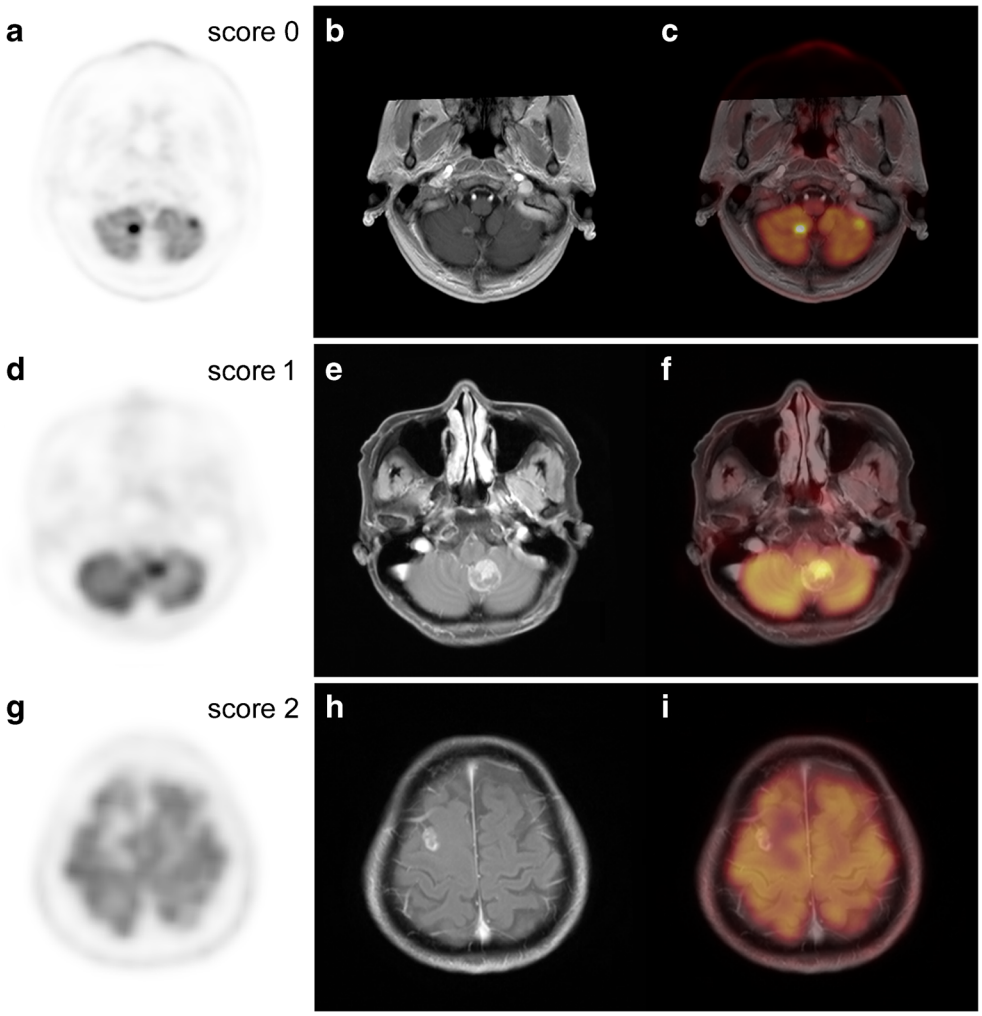

Fig. 3 Illustrative images of three patients with different molecular imaging prognostic (MIP) scores. **a**, **b**, **c** A 66-year-old female patient with a MIP score of 0 had TBR of 2.3 on PET and did not receive targeted therapy. The time to neurological progression was 9.6 months, and the patient died of disease 10.5 months after diagnosis. The corresponding Lung-molGPA score was 2.5. **d**, **e**, **f** A 60-year-old male patient with a MIP score of 1 had TBR of 4.1 on PET and was treated with afatinib and whole-brain radiotherapy. The time to neurological progression was 22.0 months, and the patient died of disease 23.0 months after diagnosis. The corresponding Lung-molGPA score was 2.0. **g**, **h**, **i** A 67-year-old male patient with a MIP score of 3 had TBR of 1.4 on PET and underwent afatinib treatment and brain radiotherapy. The time to neurological progression was 29.2 months, and the patient was alive with disease 31.8 months after diagnosis. The corresponding Lung-molGPA score was 3.0

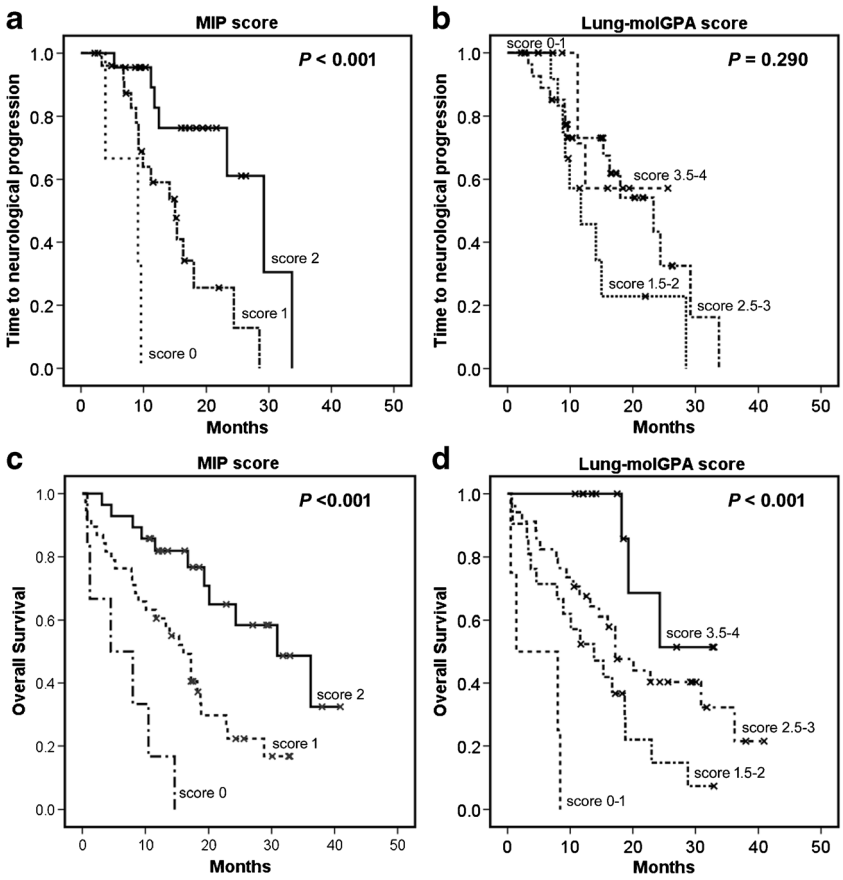

Fig. 4 Kaplan–Meier plots of time to neurological progression (nTTP) and overall survival in patients with lung adenocarcinoma and brain metastases stratified according to the molecular imaging prognostic (MIP) score (**a**, **c**) and Lung-molGPA score (**b**, **d**). Lung-molGPA scores were unable to predict nTTP

in the few reports investigating FDG-PET findings of metastatic brain tumor [28, 29], the TBR threshold of FDG-PET was not discernible from the literature. Therefore, the use of a threshold TBR value of ≥ 1.6 as a positive PET marker for brain metastases was based on previous ^{18}F-FET PET studies [24, 25]. Interestingly, in the current study, no metastatic brain tumor with TBR < 1.6 was identifiable by visual assessment on FDG-PET images. We supposed that the "imaging contrast" for tumor delineation was similar even though the radiotracers were different. Although one-third of metastases with a size < 1.0 cm were ^{18}F-FET PET-negative because of partial-volume effects, the authors did not apply a partial volume correction [24]. In our study, the smallest detected tumor had a size of 0.6 cm. It has previously been demonstrated that MRI-guided partial-volume correction can improve dynamic FDG brain data on PET/MR scanners [30]. However, the use of partial-volume correction has been occasionally avoided to prevent potential inaccuracies resulting from segmentation errors [31]. Moreover, different partial-volume correction methods for FDG-PET have led to different conclusions in relation to brain aging [32]. Here, the TBR was calculated at a single time point to determine the presence of positive or negative PET findings. Because we did not rely on changes in uptake values or dynamic data, which might need more sophisticated quantitation, we did not apply any partial volume correction. We specifically avoided complicated imaging processing methods to make our findings applicable in the clinical routine. Although the scanning time will affect FDG uptake of tumors and the averaged TBR was different between automatically coregistered images (30 min after injection) and manually coregistered images (60 min after injection), visual assessment for negative PET findings showed TBR < 1.6 in both groups. Therefore, a TBR ≥ 1.6 is appropriate in defining positive PET findings.

Herein, up to 91% of BMs originated from adenocarcinomas, a finding which is in line with a previous report [2]. It would be more cost-effective to perform brain PET/MR among NSCLC patients with a higher incidence of brain metastasis, especially for adenocarcinoma. Differently from pre-existing prognostic indexes (such as Lung-molGPA for lung adenocarcinoma) [17], we included eligibility for initial treatment with targeted therapy rather than the gene mutation status. TKI should not be invariably used in all patients with EGFR gene mutations. Because most patients with advanced lung adenocarcinomas harboring EGFR exon 20 insertion do not respond to TKI, standard chemotherapy should be considered as the first-line treatment modality [33]. The majority of patients treated with targeted therapy received afatinib, a second-generation TKI which has been shown to be more effective than first-generation TKI for treating BMs [34].

Although it is well known that the prognosis of patients with lung adenocarcinoma showing EGFR or ALK mutations and BM, who were treated by TKI, is far better than those who did not show gene mutations and were not treated by TKI, the newly proposed MIP score could further stratify patients with much better prognoses and patients with the poorest prognoses (i.e., a median OS less than half year), adding prognostic information to the use of TKI. In comparison of pre-existing prognostic indices, MIP score demonstrated OS-predicting ability comparable to that of Lung-molGPA. However, the MIP score was a significant prognostic factor for nTTP, whereas Lung-molGPA was not.

A phase-3 randomized trial demonstrated that whole-brain radiotherapy does not provide significant OS benefit for patients with NSCLC and BMs [35]. We have previously shown that afatinib can be clinically useful and provide a good response rate in treatment-naïve patients with EGFR-mutant lung adenocarcinoma and BMs regardless of whether the patient received radiotherapy [36]. The cumulative incidence of intracranial progression has been reported to be significantly lower with TKI plus radiotherapy compared with TKI alone; however, no significant differences were observed for OS [37]. Early brain radiotherapy concurrently given with TKI may improve intracranial disease control in patients with EGFR-mutant NSCLC and BMs, resulting in a survival benefit for patients with low DS-GPA scores [38]. Because the MIP score is a significant predictor of neurological progression, it might potentially serve as an ideal prognostic index for selecting appropriate candidates for brain radiotherapy.

Several limitations of our study merit comment. The retrospective nature of our investigation might be prone to a selection bias. The follow-up brain status for some patients could not be determined, and a small number of cases underwent brain radiotherapy (ultimately limiting further analyses on the impact of radiation therapy on intracranial control). As far as patients with positive ALK mutations are concerned, alectinib, which shows better activity against BMs, was unavailable at that time of analysis [39]. The brain PET/MR protocol was inconsistent, with some patients undergoing MRI on the PET/MR scanner only (i.e., without simultaneous PET acquisition). However, this situation reflects a common real-life limitation for institutes which are not equipped with PET/MR.

Conclusions

Based on a staging procedure that combines whole-body PET/CT and brain PET/MR in NSCLC, additional FDG information for metastatic brain tumors localized by contrast-enhanced MRI improves the prognostic stratification of patients with lung adenocarcinoma. The new prognostic index (MIP score)—which was obtained by combining FDG-PET findings and eligibility for initial treatment with targeted therapy—may improve the prognostic stratification of patients with lung adenocarcinoma and BMs. Because of its superior prognostic value for nTTP in comparison with the Lung-molGPA score, the MIP score might be applied to improve intracranial control and quality of life in selected cases.

Acknowledgements This study was financially supported by a grant from the Chang Gung Memorial Hospital (CMRPG3B0343), Taiwan. The authors acknowledge the statistical assistance provided by the Clinical Trial Center (MOHW107-TDU-B-212-123005), Linkou, Taiwan.

Funding This study was financially supported by a grant from the Chang Gung Memorial Hospital (CMRPG3B0343), Taiwan.

Compliance with ethical standards

Conflict of interest The authors declare no conflicts of interest.

Ethical approval All procedures performed in the study were in accordance with the ethical standards of the institutional and/or national research committee and the 1964 Helsinki Declaration (and its later amendments).

Informed consent Waiver of consent for this retrospective study was approved by the Institutional Review Board.

References

1. Schouten LJ, Rutten J, Huveneers HA, Twijnstra A. Incidence of brain metastases in a cohort of patients with carcinoma of the breast, colon, kidney, and lung and melanoma. Cancer. 2002;94:2698–705.
2. Villano JL, Durbin EB, Normandeau C, Thakkar JP, Moirangthem V, Davis FG. Incidence of brain metastasis at initial presentation of lung cancer. Neuro-Oncology. 2015;17:122–8.
3. Barnholtz-Sloan JS, Sloan AE, Davis FG, Vigneau FD, Lai P, Sawaya RE. Incidence proportions of brain metastases in patients diagnosed (1973 to 2001) in the metropolitan Detroit Cancer surveillance system. J Clin Oncol. 2004;22:2865–72.
4. Mujoomdar A, Austin JH, Malhotra R, Powell CA, Pearson GD, Shiau MC, et al. Clinical predictors of metastatic disease to the brain from non-small cell lung carcinoma: primary tumor size, cell type, and lymph node metastases. Radiology. 2007;242:882–8.
5. Goncalves PH, Peterson SL, Vigneau FD, Shore RD, Quarshie WO, Islam K, et al. Risk of brain metastases in patients with nonmetastatic lung cancer: analysis of the Metropolitan Detroit Surveillance, Epidemiology, and End Results (SEER) data. Cancer. 2016;122:1921–7.
6. National Comprehensive Cancer Network. NCCN Guidelines for Treatment of Cancer by Site: Non-Small Cell Lung Cancer. 2018 https://www.nccn.org/professionals/physician_gls/pdf/nscl.pdf.
7. Zakaria R, Das K, Bhojak M, Radon M, Walker C, Jenkinson MD. The role of magnetic resonance imaging in the management of brain metastases: diagnosis to prognosis. Cancer Imaging. 2014;14:8.
8. Yokoi K, Kamiya N, Matsuguma H, Machida S, Hirose T, Mori K, et al. Detection of brain metastasis in potentially operable non-small

cell lung cancer: a comparison of CT and MRI. Chest. 1999;115: 714–9.
9. Wessman BV, Moriarity AK, Ametlli V, Kastan DJ. Reducing barriers to timely MR imaging scheduling. Radiographics. 2014;34: 2064–70.
10. Lee SM, Goo JM, Park CM, Yoon SH, Paeng JC, Cheon GJ, et al. Preoperative staging of non-small cell lung cancer: prospective comparison of PET/MR and PET/CT. Eur Radiol. 2016;26:3850–7.
11. Heusch P, Buchbender C, Köhler J, Nensa F, Gauler T, Gomez B, et al. Thoracic staging in lung cancer: prospective comparison of 18F-FDG PET/MR imaging and 18F-FDG PET/CT. J Nucl Med. 2014;55:373–8.
12. Schwenzer NF, Schraml C, Müller M, Brendle C, Sauter A, Spengler W, et al. Pulmonary lesion assessment: comparison of whole-body hybrid MR/PET and PET/CT imaging—pilot study. Radiology. 2012;264:551–8.
13. Fraioli F, Screaton NJ, Janes SM, Win T, Menezes L, Kayani I, et al. Non-small-cell lung cancer resectability: diagnostic value of PET/MR. Eur J Nucl Med Mol Imaging. 2015;42:49–55.
14. Stelzer KJ. Epidemiology and prognosis of brain metastases. Surg Neurol Int. 2013;4:S192–202.
15. Lin X, DeAngelis LM. Treatment of brain metastases. J Clin Oncol. 2015;33:3475–84.
16. Sperduto PW, Kased N, Roberge D, Xu Z, Shanley R, Luo X, et al. Summary report on the graded prognostic assessment: an accurate and facile diagnosis-specific tool to estimate survival for patients with brain metastases. J Clin Oncol. 2012;30:419–25.
17. Sperduto PW, Yang TJ, Beal K, Pan H, Brown PD, Bangdiwala A, et al. Estimating survival in patients with lung cancer and brain metastases: an update of the graded prognostic assessment for lung cancer using molecular markers (Lung-molGPA). JAMA Oncol. 2017;3:827–31.
18. Hjorthaug K, Hojbjerg JA, Knap MM, Tietze A, Haraldsen A, Zacho HD, et al. Accuracy of 18F-FDG PET-CT in triaging lung cancer patients with suspected brain metastases for MRI. Nucl Med Commun. 2015;36:1084–90.
19. Hendriks LE, Derks JL, Postmus PE, Damhuis RA, Houben RM, Troost EG, et al. Single organ metastatic disease and local disease status, prognostic factors for overall survival in stage IV non-small cell lung cancer: results from a population-based study. Eur J Cancer. 2015;51:2534–44.
20. Paesmans M, Berghmans T, Dusart M, Garcia C, Hossein-Foucher C, Lafitte JJ, et al. Primary tumor standardized uptake value measured on fluorodeoxyglucose positron emission tomography is of prognostic value for survival in non-small cell lung cancer: update of a systematic review and meta-analysis by the European Lung Cancer working Party for the International Association for the study of lung cancer staging project. J Thorac Oncol. 2010;5:612–9.
21. Na F, Wang J, Li C, Deng L, Xue J, Lu Y. Primary tumor standardized uptake value measured on F18-fluorodeoxyglucose positron emission tomography is of prediction value for survival and local control in non-small-cell lung cancer receiving radiotherapy: meta-analysis. J Thorac Oncol. 2014;9:834–42.
22. Varrone A, Asenbaum S, Vander Borght T, Booij J, Nobili F, Nagren K, et al. EANM procedure guidelines for PET brain imaging using [18F]FDG, version 2. Eur J Nucl Med Mol Imaging. 2009;36:2103–10.
23. Aasheim LB, Karlberg A, Goa PE, Haberg A, Sorhaug S, Fagerli UM, et al. PET/MR brain imaging: evaluation of clinical UTE-based attenuation correction. Eur J Nucl Med Mol Imaging. 2015;42:1439–46.
24. Unterrainer M, Galldiks N, Suchorska B, Kowalew LC, Wenter V, Schmid-Tannwald C, et al. (18)F-FET PET uptake characteristics in patients with newly diagnosed and untreated brain metastasis. J Nucl Med. 2017;58:584–9.
25. Gempt J, Bette S, Buchmann N, Ryang YM, Forschler A, Pyka T, et al. Volumetric analysis of F-18-FET-PET imaging for brain metastases. World Neurosurg. 2015;84:1790–7.
26. Edge SB, Byrd DR, Compton CC, Fritz AG, Greene FL, Trotti A, editors. AJCC cancer staging manual. 7th ed. New York, NY: Springer; 2010.
27. Diaz ME, Debowski M, Hukins C, Fielding D, Fong KM, Bettington CS. Non-small cell lung cancer brain metastasis screening in the era of positron emission tomography-CT staging: current practice and outcomes. J Med Imaging Radiat Oncol. 2018;62: 383–8.
28. Kruger S, Mottaghy FM, Buck AK, Maschke S, Kley H, Frechen D, et al. Brain metastasis in lung cancer. Comparison of cerebral MRI and 18F-FDG-PET/CT for diagnosis in the initial staging. Nuklearmedizin. 2011;50:101–6.
29. Lee HY, Chung JK, Jeong JM, Lee DS, Kim DG, Jung HW, et al. Comparison of FDG-PET findings of brain metastasis from non-small-cell lung cancer and small-cell lung cancer. Ann Nucl Med. 2008;22:281–6.
30. Yan J, Lim JC, Townsend DW. MRI-guided brain PET image filtering and partial volume correction. Phys Med Biol. 2015;60:961–76.
31. Villemagne VL, Pike KE, Chetelat G, Ellis KA, Mulligan RS, Bourgeat P, et al. Longitudinal assessment of Abeta and cognition in aging and Alzheimer disease. Ann Neurol. 2011;69:181–92.
32. Greve DN, Salat DH, Bowen SL, Izquierdo-Garcia D, Schultz AP, Catana C, et al. Different partial volume correction methods lead to different conclusions: an (18)F-FDG-PET study of aging. NeuroImage. 2016;132:334–43.
33. Naidoo J, Sima CS, Rodriguez K, Busby N, Nafa K, Ladanyi M, et al. Epidermal growth factor receptor exon 20 insertions in advanced lung adenocarcinomas: clinical outcomes and response to erlotinib. Cancer. 2015;121:3212–20.
34. Hoffknecht P, Tufman A, Wehler T, Pelzer T, Wiewrodt R, Schutz M, et al. Efficacy of the irreversible ErbB family blocker afatinib in epidermal growth factor receptor (EGFR) tyrosine kinase inhibitor (TKI)-pretreated non-small-cell lung cancer patients with brain metastases or leptomeningeal disease. J Thorac Oncol. 2015;10:156–63.
35. Mulvenna P, Nankivell M, Barton R, Faivre-Finn C, Wilson P, McColl E, et al. Dexamethasone and supportive care with or without whole brain radiotherapy in treating patients with non-small cell lung cancer with brain metastases unsuitable for resection or stereotactic radiotherapy (QUARTZ): results from a phase 3, non-inferiority, randomised trial. Lancet. 2016;388:2004–14.
36. Li SH, Liu CY, Hsu PC, Fang YF, Wang CC, Kao KC, et al. Response to afatinib in treatment-naive patients with advanced mutant epidermal growth factor receptor lung adenocarcinoma with brain metastases. Expert Rev Anticancer Ther. 2018;18:81–9.
37. Sung S, Lee SW, Kwak YK, Kang JH, Hong SH, Kim YS. Intracranial control and survival outcome of tyrosine kinase inhibitor (TKI) alone versus TKI plus radiotherapy for brain metastasis of epidermal growth factor receptor-mutant non-small cell lung cancer. J Neuro-Oncol. 2018;139:205–13.
38. Liu Y, Deng L, Zhou X, Gong Y, Xu Y, Zhou L, et al. Concurrent brain radiotherapy and EGFR-TKI may improve intracranial metastases control in non-small cell lung cancer and have survival benefit in patients with low DS-GPA score. Oncotarget. 2017;8: 111309–17.
39. Gadgeel SM, Gandhi L, Riely GJ, Chiappori AA, West HL, Azada MC, et al. Safety and activity of alectinib against systemic disease and brain metastases in patients with crizotinib-resistant ALK-rearranged non-small-cell lung cancer (AF-002JG): results from the dose-finding portion of a phase 1/2 study. Lancet Oncol. 2014;15:1119–28.